Articles

Role of the HIV gp120 Conserved Domain 5 in Processing and Viral Entry[†]

Jayita Sen,[‡] Amy Jacobs,[§] and Michael Caffrey*[,‡]

Department of Biochemistry and Molecular Genetics, University of Illinois at Chicago, Chicago, Illinois 60607, and Center for Cancer Research Nanobiology Program, NCI-Frederick, Frederick, Maryland 21702

Received February 7, 2008; Revised Manuscript Received June 3, 2008

ABSTRACT: The importance of the HIV gp120 conserved domain 5 (gp120-C5) to envelope function has been examined by alanine scanning mutagenesis and subsequent characterization of the mutagenic effects on viral entry and envelope expression, processing, and incorporation, as well as gp120 association with gp41. With respect to the wild-type gp120, mutational effects on viral entry fall into three classes: (1) functional (V489A, E492A, P493A, T499A, K500A, K502A, R503A, R504A, V505A, and V506A; (2) nonfunctional (I491A, L494A, V496A, and P498A); (3) enhanced (K490A, G495A, and Q507A). The nonfunctionality of the mutants is attributed to a combination of deleterious effects on processing, gp120−gp41 association, and membrane fusion. In the case of the nonfunctional mutant P498A, the introduction of the SOS mutation (A501C/T601C) results in substantially increased envelope processing and a gain of function. The effects of the mutants are interpreted with respect to the structures of gp41 and gp120. The extent of sensitivity of gp120-C5 to alanine substitutions underscores the importance of this domain to envelope function and suggests that gp120-C5 is an attractive and novel target for future drug discovery efforts.

The viral envelope proteins gp120 and gp41 play critical roles in human immunodeficiency virus (HIV)[1] entry (reviewed in ref *1*). gp120 and gp41 are formed by cleavage of the precursor gp160 by cellular furin-like proteases (*2*). gp120 and gp41 remain associated as a noncovalent complex on the viral surface with gp120 mediating attachment of the virus to the appropriate target cells through interactions with CD4 and chemokine coreceptors (*3, 4*) and gp41 mediating fusion of the viral and target cell membranes, thereby allowing entry of the viral genetic material. The indispensable roles of gp120 and gp41 suggest that they present attractive targets for novel antiviral therapies.

The native structure of the gp41−gp120 complex is not known; however, there is a significant amount of structural information available for isolated domains of the HIV envelope proteins or their analogues in SIV (simian immunodeficiency virus). For example, there is extensive information on the extracellular domains, or ectodomains, of HIV and SIV gp41 from X-ray, NMR, and molecular modeling studies (*5*–*12*). Moreover, there are X-ray structures of the HIV and SIV gp120 core domain bound to CD4 (*13, 14*) and in the free state (*15*). Unfortunately, the gp120 core structure is missing large regions of the conserved domains 1 and 5 (gp120-C1 and gp120-C5, respectively), which have been implicated by mutagenesis studies to directly interact with gp41 (*16*−*18*). However, the structure of HIV gp120 conserved domain 5 (gp120-C5) has been determined as an isolated domain by NMR spectroscopy (*19*). Of special note are the studies of Binley et al. (*18*), who performed cysteine scanning mutagenesis of gp120-C5 with the loop of gp41 to elucidate potential sites of intermolecular interactions. The most reactive cysteine pair formed a disulfide bond between positions A501 of gp120-C5 and T605 of the gp41 loop, which suggested that these regions were in close proximity in the gp120−gp41 complex (*18*). Importantly, this mutant, called SOS, was reported to be an antigenic mimic of the virion associated envelope trimer (*18*). In the present study, we report the first systematic mutation study of the importance of HIV gp120-C5 residues to envelope function with the long-term goal of identifying gp120 regions that are attractive sites for drug intervention.

EXPERIMENTAL PROCEDURES

Mutagenesis and Viral Entry Assays. Mutants were prepared from plasmid pHXB2 (*20*) using the Stratagene QuikChange II site-directed mutagenesis kit with subsequent verification by DNA sequencing. The functionality of gp120 mutants was determined in a luciferase-based entry assay (*21*). For this assay, plasmids pHXB2 (bearing wild type or mutant gp120) and pNL4-3.Luc.R-E- (*21*) were cotransfected by calcium phosphate precipitation into 293T cells, which

[†] This work was partially supported by NIH Grant RO1 AI47674 to M.C.

* To whom correspondence should be addressed. Tel: (312) 996-4959. Fax: (312) 413-0353. E-mail: caffrey@uic.edu.

[‡] University of Illinois at Chicago.

[§] NCI-Frederick.

[1] Abbreviations: HIV, human immunodeficiency virus; NMR, nuclear magnetic resonance.

10.1021/bi800227z CCC: $40.75
Published on Web 07/03/2008

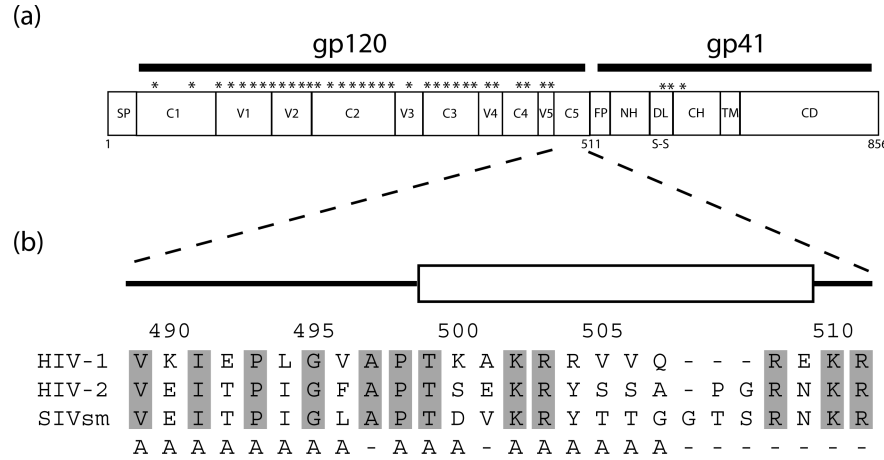

FIGURE 1: (a) Organization of HIV envelope proteins (*23*). Putative glycosylation sites are denoted by asterisks. Domain abbreviations: SP (signal peptide), C1−C5 (conserved domains 1 to 5), V1−V5 (variable domains 1 to 5), FP (fusion peptide), NH (N helix), DL (disulfide loop), CH (C helix), TM (transmembrane domain), and CD (cytoplasmic domain). (b) Amino acid sequence alignment of HIV-1, HIV-2, and SIV_{sm} gp120-C5 (*23*). Conserved residues of gp120-C5 are highlighted by gray shading. Residues that are substituted by alanine in the present study are denoted below. Numbering corresponds to that of HIV-1 HXB2. Secondary structure is taken from Guilhaudis et al. (*19*).

were maintained in Dulbecco's medium with 10% FBS, 1% L-glutamine, 1% penicillin−streptomycin, and 0.5 mg/mL G418. Forty-eight hours posttransfection, the medium was harvested and filtered through a 0.45 μm filter to make the virus stock. For assay of viral entry, U87.CD4.CXCR4 cells (*4*), which were maintained in Dulbecco's medium with 15% FBS supplemented with 1 μg/mL puromycin, 300 μg/mL G418, 1% L-glutamine, and 1% penicillin−streptomycin, were seeded to 1×10^5 cells/well of a 12-well cell culture plate in a volume of 1 mL. The following day, 500 μL of the virus stock was added to each of the wells of the U87 cells after removal of the medium. The plates were incubated overnight at 37 °C in a CO_2 incubator. After approximately 16 h, the virus was aspirated and replaced with U87 medium, and the cells were allowed to rest for another 24 h. Luciferase activity was measured using the luciferase assay system from Promega and a Berthold FB12 luminometer running Sirius software. The experiments were run in triplicate from transfection to assay of luciferase activity, and thus the uncertainties represent all stages of the experiment. In all cases, the entry levels fell within the linear range of detection (i.e., the values of the wild type and mutants never exceeded 3×10^6 relative light units). The reported luciferase activities have been normalized to p24 levels.

Western Blot Analysis. Cell lysates were collected from 293T producer cells using lysis buffer (50 mM Tris, pH 7.5, 150 mM NaCl, 5 mM EDTA, 0.5% NP-40, and 0.1% SDS). Prior to electrophoresis, the cell lysates were normalized for total protein concentration using the Bradford protein assay kit (Bio-Rad). The virus pellet was prepared by ultracentrifugation on a cushion of 20% sucrose at 55000 rpm for 1 h using a Beckman SW55Ti rotor. The virus pellets were resuspended in lysis buffer (50 mM Tris, pH 7.5, 150 mM NaCl, 5 mM EDTA, 0.5% NP-40, and 0.1% SDS). After SDS−PAGE, transfer, and blocking the membranes with 5% milk/TBST for gp41 and SuperBlock (Pierce) for gp120, the blots were probed with either goat anti-HIV-1 gp120 polyclonal antibody (United States Biological) or with mouse anti-HIV-1 gp41 monoclonal antibody (Chessie 8; NIH AIDS Research and Reference Reagent Program (*22*)). The secondary antibody used was peroxidase-conjugated AffiniPure donkey anti-goat or goat anti-mouse IgG (H+L) from Jackson ImmunoResearch Laboratories, Inc., and developed using the ECL kit (Amersham). The relative amount of envelope on the Western blots was determined by a densitometric analysis. Briefly, digital scans of the blots were opened in Photoshop 7.0, the image was inverted, the appropriate bands were selected with the Lasso function, and the mean intensity and area were measured with the Histogram function. Subsequently, the relative percent was determined by the relationship: (100 × mean intensity × area)/(wild-type mean intensity × wild-type area).

Immunofluorescence Flow Cytometry. 293T cells were treated with sCD4 (4 μg/mL) on ice, washed twice, and incubated with anti-CD4 antibody (OKT4) on ice. After two washes and fixing with 1% paraformaldehyde on ice, cells were washed again, stained with antimouse IgG-FITC (against OKT4), and analyzed by flow cytometry (DakoCytomation CyAn ADP).

RESULTS

Design of the HIV gp120-C5 Mutants. The organization of the HIV envelope proteins is shown in Figure 1a. As shown by Figure 1b, gp120-C5 is relatively conserved between HIV-1, HIV-2, and SIV with ∼50% sequence identity (*23*). In the NMR structure of gp120-C5, residues 489−498 are in a turn structural motif, and residues 499−509 form a helix (*19*). With respect to HIV-1, gp120-C5 of HIV-2 and SIV_{sm} exhibit insertions at the end of the helix in the region before the furin recognition site (sequence = REKR, residues 508−511). In the present study 17 alanine substitutions of HIV-1 gp120-C5 were generated by site-directed mutagenesis (Figure 1b). Note that the residues comprising the recognition site for furin processing (i.e., residues 508−511) have not been mutated, in order to obviate any problems with envelope processing (*24–26*).

Viral Entry of the HIV gp120-C5 Mutants. The effects of the gp120 mutations on viral entry were first tested by a luciferase-based assay, in which viral entry is proportional to the observed luciferase activity (*21*, *27*, *28*). As shown in Figure 2a, the viral entry (as measured by luciferase activity)

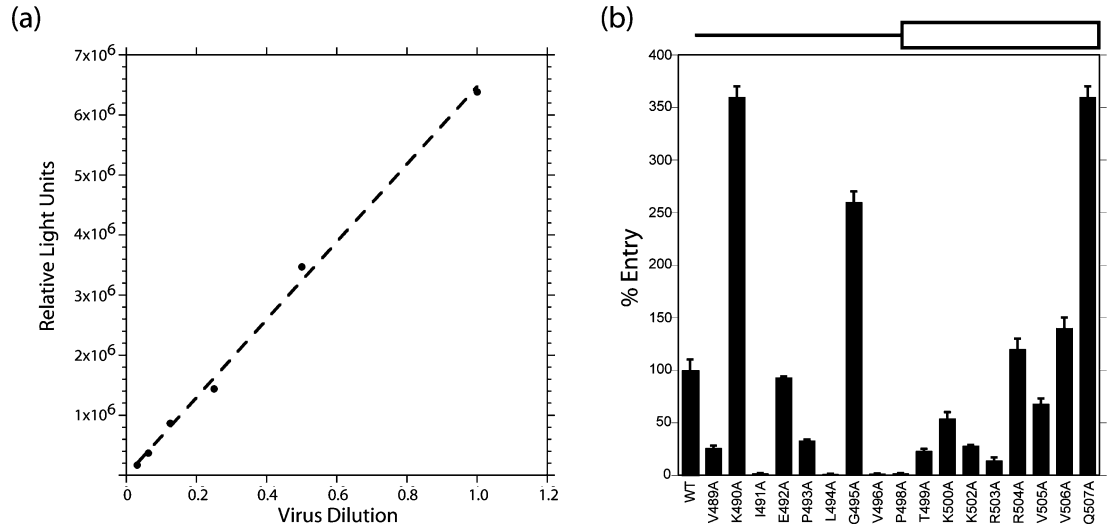

FIGURE 2: (a) Viral entry as a function of sequential dilutions of the pseudovirus stock expressing wild-type envelope. The dotted line corresponds to a linear regression of the data ($R^2 = 0.997$). (b) Mutational effects on viral entry with respect to the wild type, based on the luciferase reporter assay for entry into U87.CD4.CXCR4 cells. Viral entry has been normalized to p24 levels. The error bars represent the standard deviation of three separate experiments. Secondary structure taken from Guilhaudis et al. (*19*).

Table 1: Summary of Viral Entry and Level of Envelope Detected in Cell Lysates and Virus of Wild-Type and Alanine Mutants of HIV gp120-C5[a]

mutant	entry (% WT)	cell gp160	cell gp120	cell gp41	virus gp160	virus gp120	virus gp41
WT	100 ± 10	++	++	++	++	++	++
V489A	26 ± 2	+++	+++	++	+++	++	++
K490A	360 ± 10	+++	+++	++	++	++	++
I491A	1.7 ± 0.2	+++	+	++	+++	++	++
E492A	93 ± 1	++	++	++	+	+	+
P493A	33 ± 1	+++	++	++	++	+	++
L494A	1.3 ± 0.1	+++	+	++	+++	−	+
G495A	260 ± 10	+++	+++	++	++	++	++
V496A	1.6 ± 0.1	+++	+	+	+++	+	+
P498A	1.8 ± 0.1	+++	−	−	++	−	−
T499A	23 ± 2	+++	++	++	+++	+	+
K500A	54 ± 6	+++	+++	+++	+++	++	++
K502A	28 ± 1	++	++	++	++	++	++
R503A	14 ± 3	++	+++	++	++	++	++
R504A	120 ± 10	++	++	++	+++	+	++
V505A	68 ± 5	++	++	++	+++	++	++
V506A	140 ± 10	+++	+++	++	+++	+	++
Q507A	360 ± 10	+++	++	++	++	+	++

[a] Entry levels have been normalized to virus p24 amounts and are reported as the % entry with respect to the wild-type virus. The reported errors correspond to the standard deviation of three separate experiments. For Western analysis of cell lysates, equivalent amounts of total protein were analyzed. For Western analysis of virus, equivalent amounts of p24 were analyzed. Envelope levels are based on a densitometric analysis of Western blots, where − = <20%, + = 20−60%, ++ = 60−140%, and +++ > 140%.

is linearly proportional to the amount of wild-type pseudovirus added to U87.CD4.CXCR4 cells over a range from 100000 to 7000000 relative light units (R^2 of the linear regression is 0.997). As shown in Figure 2b and summarized in Table 1, the effects of the mutations range from nearly complete abolishment of viral entry (e.g., L494A) to significant enhancement of viral entry (e.g., K490A). The mutants can be divided into three categories: (1) functional (defined as 10−140% of wild-type entry; (2) nonfunctional (defined as <2% of wild-type entry); (3) enhancement of viral entry (defined as >200% of wild-type entry). Category 1 mutants, those that are defined as functional, include V489A, E492A, P493A, T499A, K500A, K502A, R503A, R504A, V505A, and V506A. In general, this class of mutants is a mixture of conserved and nonconserved residues spread throughout the sequence (Figure 1b). Interestingly, V489, P493, T499, K502, and R503, which are conserved in HIV-2 and SIV gp120, are functional for viral entry. Category 2 mutants, defined as nonfunctional, include I491A, L494A, V496A, and P498A. In all four cases, substitution by alanine results in a relatively radical change in the nature of the amino acid side chain, and thus the significant effects could be anticipated. Of this group I491 and P498 are conserved among gp120, and hydrophobicity is conserved at positions 494 and 496 (Figure 1b). Category 3 mutants, those that enhance viral entry, include K490A, G495A, and Q507A, of which G495 is conserved among gp120 (Figure 1b).

Mutant Expression, Processing, Viral Incorporation, and Association with gp41. The effects of the HIV gp120-C5 mutations on viral entry could be due to a number of factors: (i) reduced envelope expression or stability; (ii) inefficient processing of the precursor gp160; (iii) reduced incorporation of envelope into the virus; (iv) decreasing the affinity of the interaction between gp41 and gp120, thereby resulting in dissociation (or "shedding") of gp120 into the media; (v) the formation of a gp41−gp120 complex that cannot support the attachment or fusion steps of viral entry. On the other hand, mutational enhancement of viral entry could be due

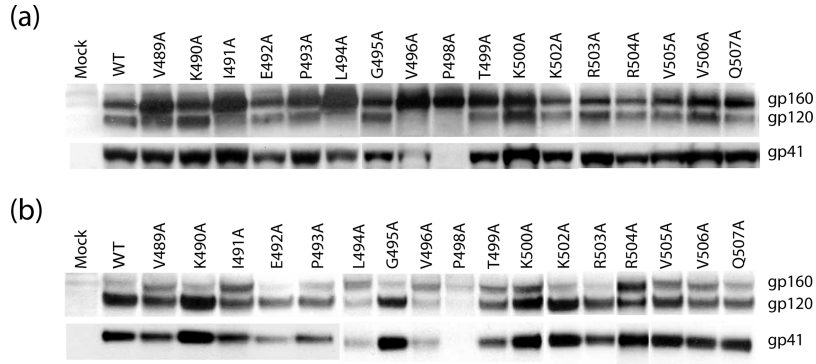

FIGURE 3: Western blot analysis of envelope expression, processing, and gp120−gp41 association for HIV wild type and the gp120-C5 mutants in cell lysates (a) and virus (b) from 293T cells. For the cell lysates, equivalent amounts of total protein have been analyzed; for the virus, equivalent amounts of p24 have been analyzed.

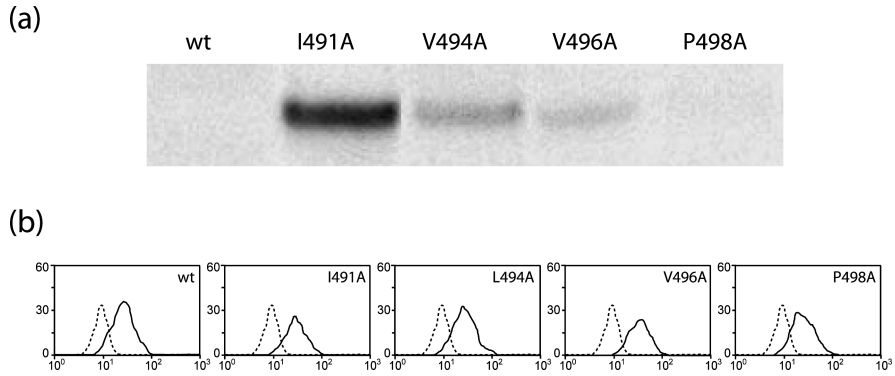

FIGURE 4: Conformational and surface expression properties of the HIV gp120-C5 nonfunctional mutants. (a) Shedding of wild-type and mutant envelope, based on Western blot analysis of gp120 found in the media of 293T cells. (b) Surface expression of wild-type and mutant envelope, based on an immunofluorescence flow cytometry assay of sCD4 binding to 293T cells. The dotted lines correspond to mock transfected cells treated in the same manner as the cells expressing envelope.

to (i) increased envelope expression, processing, stability, or viral incorporation resulting in increased concentration of envelope proteins at the virus surface, (ii) enhancement of the gp120-mediated viral attachment step, and (iii) enhancement of the gp41-mediated membrane fusion step. Many of these scenarios can be distinguished by a Western blot analysis of envelope present in cell lysates expressing wild-type and mutant gp120 and the virus produced by these cells. For example, the presence of gp41 in virus demonstrates expression, processing, and incorporation into the virus, and the presence of gp120 in cell lysates and virus indicates that gp120 is associated with gp41 and not significantly shed into the medium. In Figure 3a Western blot analysis of the wild-type and mutant gp120 present in cell lysates and virus is shown, and a summary of the results is presented in Table 1. In the case of the wild-type, the gp120 and gp41 are clearly present in the cell lysates and viral particles, and thus envelope is expressed, processed, and incorporated into virus, and gp120 remains associated with gp41, as expected. The category 1 mutants (V489A, E492A, P493A, T499A, K500A, K502A, R503A, R504A, V505A, and V506A), those that are functional, exhibit a pattern of envelope proteins that is similar to the wild type. However, many of these mutants (V489A, T499A, K500A, R504A, V505A, and V506A) also exhibit increased levels of gp160 incorporation into virus (Figure 3, Table 1), suggesting that they may have decreased envelope processing by furin. Somewhat surprisingly, the nonfunctional mutants I491A, L494A, and V496A exhibit gp120 and gp41 profiles (Figure 3, Table 1), suggesting that these mutants are expressed, processed, and incorporated into virus and have not caused discernible dissociation of gp120. However, the presence of gp160 in virus indicates that the mutations have decreased levels of envelope processing (Figure 3, Table 1). In marked contrast, the absence of gp120 and gp41 in cell lysates and virus of the nonfunctional mutant P498A suggests that the mutation abrogates processing. Finally, the category 3 mutants (K490A, G495A, and Q507A), those that exhibit enhanced viral entry, show an envelope profile that is similar to the wild type. Consequently, their enhancement does not appear to be due to increased expression, processing, viral incorporation, and gp41 association, and thus their increased entry is presumably due to altered binding of receptors and/or enhanced fusion of the viral and cellular membranes.

Ligand Binding Properties of the Nonfunctional gp120-C5 Mutants. The gp41−gp120 interface of the nonfunctional mutants (category 2) was next probed by Western blot analysis of the supernatants derived from cells producing envelope. As shown in Figure 4a, mutant I491A in particular, as well as mutants L494A and V496A, exhibits significant amounts of gp120 in the supernatant with respect to the wild type, suggesting that these mutations have destabilized the association of gp120 with gp41. Dissociation of gp120 may result from direct or indirect effects of the mutation on the gp120−gp41 interaction. Moreover, in the absence of structural data, the magnitude of the mutational effects on conformation is currently unknown. Not unexpectedly, P498A, which was not processed (cf. discussion above), is not observed in the supernatant. Next, using sCD4 the cell

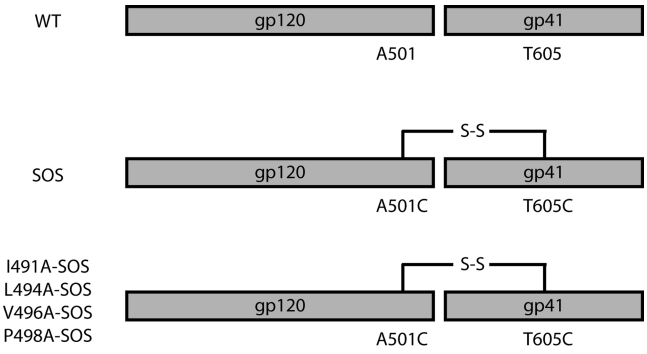

FIGURE 5: Schematic representation of the SOS mutations. SOS corresponds to the double mutation A501C/T605C (*18*). In the cases of the nonfunctional mutants, the SOS mutation (A501C/T605C) has been added to result in triple mutations. The potential intermolecular disulfide bond of the SOS mutation is denoted by a solid line.

surface expression levels of the nonfunctional mutants were assayed by immunofluorescence flow cytometry. Binding to sCD4 is also indicative of the global structural integrity of gp120 and/or gp160 (*29*); however, the gp120-C5 domain is distant from the CD4 binding site, and thus in the present case sCD4 binding is most appropriate as an assay of envelope surface expression. Cells expressing envelope protein were treated or mock-treated with sCD4 and subsequently to a FITC-conjugated secondary antibody (OKT4) that binds to CD4. FITC acquisition in the flow cytometer indicates binding of sCD4 to the gp120 and/or gp160 present on the cell surface. As shown in Figure 4b, all of the nonfunctional mutants exhibit similar levels of sCD4 binding, with respect to the wild type. Thus, the gp120-C5 nonfunctional mutants are expressed at the surface at levels comparable to wild-type envelope, suggesting that the mutants are properly folded to pass the ER quality control.

SOS Mutations of the gp120-C5 Nonfunctional Mutants. Recently, we have suggested that the gp120−gp41 interaction plays an important role in processing of gp160 (*28*). As discussed above, the nonfunctional mutants exhibit decreased processing by furin. Furthermore, mutants I491A, L494A, and V496A appear to decrease the affinity of gp120 for gp41. To test whether the decreased processing of the nonfunctional mutants is due to alteration of the gp120−gp41 interaction in gp160, we generated a series of SOS mutants (i.e., they are triple mutations with A501C and T605C substitutions), as outlined in Figure 5. In the simplest scenario, lack of disulfide bond formation in the triple mutant, which normally occurs in the SOS mutant (*18*), would suggest that the mutation has altered the envelope structure to an extent that the A501 region of gp120-C5 is no longer in a position to interact with the T605 region of the gp41 loop. Such an observation would support the hypothesis that the gp120-C5−gp41 loop interaction is present in gp160 and is required for efficient furin processing (*28*) and would also explain the weakened gp120−gp41 association exhibited by many of the mutants. The effects of the SOS mutations on viral entry were probed by the luciferase-based viral entry assay in the presence and absence of reducing agent as shown in Figure 6a and summarized in Table 2. In the case of the SOS mutant, the mutation is nonfunctional for entry (i.e., <1% of wild type); however, function is gained back in the presence of reductant, as previously documented (*30, 31*).

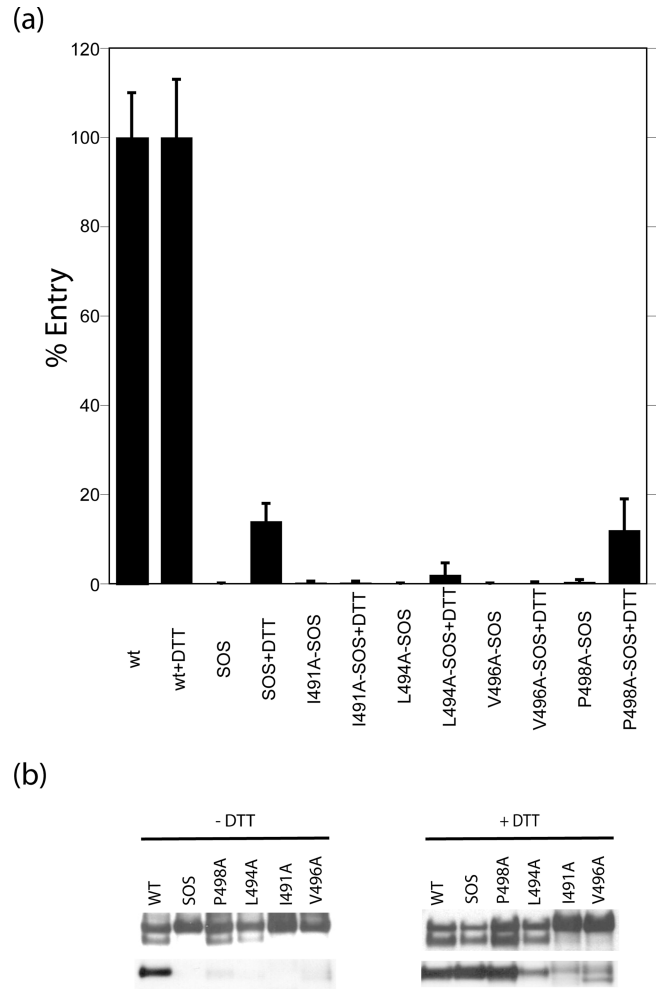

FIGURE 6: Effects of the SOS mutations on I491A, L494A, V496A, and P498A. (a) Mutant effects on viral entry, based on the pseudovirus assay. Error bars represent the standard deviation of three separate experiments. (b) Mutant effects on expression, processing, and gp120−gp41 association, based on Western blot analysis of 293T cell lysates in the presence and absence of DTT.

Table 2: Summary of Viral Entry and Level of Envelope Detected in Cell Lysates of Wild-Type and Mutants of HIV gp120-C5[a]

mutant	entry (% WT)	cell gp160	cell gp120	cell gp41
WT	100 ± 10	++	++	++
WT + DTT	100 ± 13	++	++	++
SOS	0.1 ± 0.1	++	−	−
SOS + DTT	14 ± 4	++	++	++
I491A-SOS	0.3 ± 0.3	++	−	−
I491A-SOS + DTT	0.3 ± 0.3	+++	−	+
L494A-SOS	0.1 ± 0.1	++	+	−
L494A-SOS + DTT	2.0 ± 2.7	++	++	+
V496A-SOS	0.1 ± 0.1	++	−	−
V496A-SOS + DTT	0.2 ± 0.2	+++	−	+
P498A-SOS	0.4 ± 0.5	++	++	−
P498A-SOS + DTT	12 ± 7	+++	++	++

[a] Entry levels have been normalized to virus p24 amounts and are reported as the amount with respect to the wild-type virus in the presence or absence of 25 mM DTT. Note that the wild-type entry is reduced by ~50% in the presence of 25 mM DTT, which is presumably due to reduction of native disulfide bonds found within the HIV envelope. For analysis of cell lysates, equivalent amounts of total protein were analyzed. Envelope levels are based on a densitometric analysis of Western blots, where − = <20%, + = 20−60%, ++ = 60−140%, and +++ > 140%.

In the cases of I491A-SOS, L494A-SOS, and V496A-SOS, introduction of the two cysteines does not restore activity

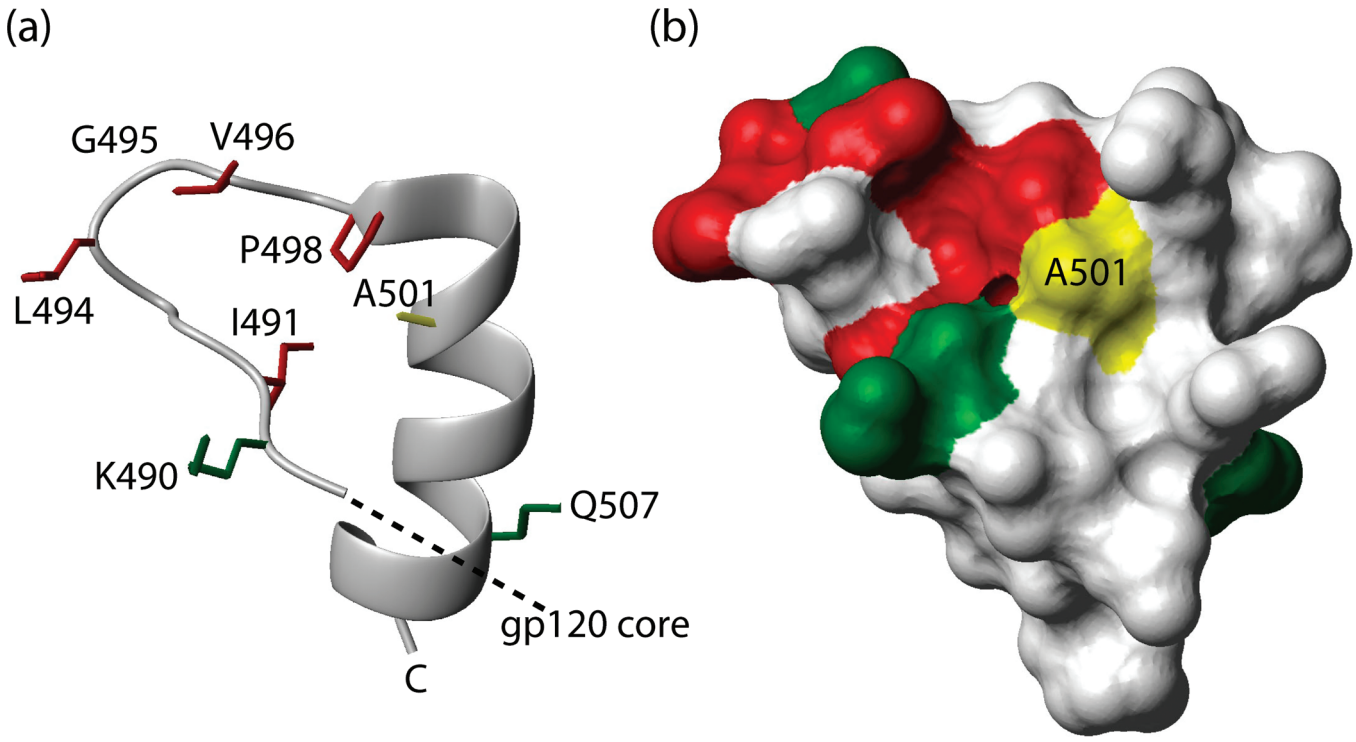

FIGURE 7: (a) Location of mutant sites in a ribbon representation of the HIV gp120-C5. (b) Location of the mutant sites on the surface of HIV-gp120-C5. Both figures are in an identical orientation. In each case, mutation sites that significantly decrease viral entry (i.e., exhibit <2% entry with respect to the wild type) are colored red, and mutation sites that increase viral entry (i.e., exhibit >200% entry with respect to the wild type) are colored green. The site of the SOS mutation site is denoted in yellow. Coordinates of HIV gp120-C5 were taken from Guilhaudis et al. (*19*).

under oxidizing or reducing conditions. In contrast, P498A-SOS gains function upon the addition of reducing agent, suggesting that the A501C−T605C disulfide bond forms and that formation of this disulfide bond partially overcomes the deleterious effects of the P498A substitution. Envelope processing and gp120−gp41 association were further probed by Western blot analysis of the SOS mutant cell lysates (Figure 6b). In the case of SOS, gp120 and gp41 are only observed under reducing conditions supporting the presence of the A501C−T605C disulfide bond (cf. refs *18* and *30*). In the cases of I491A-SOS and V496A-SOS, only small levels of gp41 are observed in the presence of reductant, which suggests that introduction of the two cysteines has significantly disrupted gp160 processing with respect to the single site mutations (compare Figure 3a with Figure 6b). The second smaller gp41 band of V496A-SOS observed in Figure 6b is presumably due to increased proteolysis. In the case of L494A-SOS, the presence of gp120 and gp41 upon reduction indicates that the SOS disulfide forms; however, the mutant is still nonfunctional for viral entry, suggesting that the reestablishment of processing does not overcome the deleterious effect of the L494A substitution. Finally, P498A-SOS, the mutant that gains function in the viral entry assay, exhibits significant amounts of gp120 and gp41 upon reduction, suggesting that the SOS disulfide forms and, in marked contrast to the single site mutation, that processing occurs.

DISCUSSION

Previous Studies of gp120-C5 Mutants. A number of previous studies have characterized the effects of single-site mutations in HIV gp120-C5 on viral function, and thus it is of interest to compare the conclusions of these studies in light of the present work. For example, Bosch and Pawlita (*26*) showed that mutants K500N, K502N, and R504S (basic side chains substituted by neutral side chains) were processed properly, which is an observation in agreement with the equivalent alanine substitutions presented herein (cf. Table 1). Helseth et al. (*17*) showed that I491F, P493K, and G495K disrupted association with gp41. In the present study, the alanine substitutions of the equivalent residues are shown not to disrupt association with gp41, as evidenced by the presence of gp120 in the viral pellets (Figure 3b, Table 1). In the case of I491, the differences may suggest that the steric properties of phenylalanine are more disruptive to the complex than alanine. In the cases of P493 and G495, the observed differences are presumably due to substitution by alanine, a small neutral residue, in contrast to substitution by lysine, a bulky positively charged residue. Nonetheless, mutants I491A and G495A exhibit significant effects on viral entry, consistent with the notion that these residues are important to envelope function. Finally, we note that the present study represents the first single site mutations to residues V489, K490, E492, L494, V496, P498, T499, R503, V505, V506, and Q507. Of the novel mutations, mutants L494A, V496A, P498A, and R503A exhibit significantly impaired function, and mutants K490A and Q507A exhibit significantly enhanced viral entry with respect to wild-type gp120.

The gp120–gp41 Interface. As discussed in the introduction, the studies of Binley et al. (*18*) have led to significant insight into the gp120−gp41 interface. In their study, pairs of non-native cysteines were introduced into the regions of the HIV gp41 loop and gp120-C5 that are thought to form

the interaction site, and the presence of an intermolecular disulfide bond was taken to indicate close proximity of the respective gp41 and gp120 residues. The most responsive site of HIV gp120-C5, and thus presumably a site that is directly interacting with gp41, was found at position 501 and other less responsive sites were found at positions 493, 495, 497, 498, and 499 (*18*). Interestingly, in our study mutant G495A exhibits enhanced viral entry with respect to the wild type, making it tempting to speculate that this mutation has enhanced viral entry by perturbing the gp41−gp120 interface to a conformation that favors receptor binding and/or membrane fusion. On the other hand, P498A of the present study is nonfunctional due to a lack of processing. Moreover, mutants P493A and T499A exhibit significantly reduced viral entry; however, neither of these mutants results in discernible dissociation of gp41 from gp120, based on the presence of gp120 in virus (Figure 3, Table 1). Strikingly, introduction of the SOS mutation into the P498A background results in furin processing and a gain of function (Figure 6, Table 2). Thus, the presence of the SOS bond in P498A apparently does not disrupt a favorable interaction between gp120-C5 and the gp41 loop, thereby orienting the gp120-C5 furin recognition site for processing of gp160. The observation that gp120-C5 directly interacts with the gp41 loop in P498A-SOS is consistent with the notion that these domains interact in gp160, as previously suggested (*28*).

Location of Mutants within gp120. As noted above, there is a high-resolution structure of the HIV gp120-C5 as an isolated domain from NMR studies; however, it is important to note that the NMR structure was determined in the presence of 40% trifluoroethanol, a cosolvent that stabilizes helical structure (*19*). Moreover, the NMR structure was determined in the absence of gp120 and gp41 domains that are thought to interact with gp120-C5 (*19*). Nonetheless, it is of interest to consider the location of the mutations in the structure of gp120-C5 with the above-noted caveats. In Figure 7, ribbon and space-filling representations of HIV gp120-C5 are shown. In this figure, the mutants that abrogate function (I491A, L494A, V496A, and P498A) are colored red, and the mutants that enhance function (K490A, G495A, and Q507A) are colored green. In addition, the site of the SOS mutation within gp120-C5 (A501) is shown in yellow and is taken to mark an area of direct interaction between gp120 and gp41. With the exception of Q507, the largest mutational effects are centered around A501, which is consistent with the notion that the mutations directly affect the gp120−gp41 interaction. However, note that mutational effects could also be propagated from sites that are distant to the gp120−gp41 interaction. The nonfunctional mutants are clearly located in close proximity within the "hydrophobic elbow" of gp120-C5 (*19*). In the wild type, a hydrophobic contact occurs between the side chains of conserved residues I491 and P498 that presumably stabilizes the turn element. Substitution by alanine would be expected to significantly impair this interaction, and thus the deleterious effects of I491A and P498A are not surprising. On the other hand, L494 and V496 are more surface exposed, suggesting that they make hydrophobic contacts with other domains of gp120 or gp41. The increased shedding of L494A and V496A (cf. Figure 4) supports this idea. In the cases of the mutants that exhibit enhanced function, K490 and G495 are in close proximity to the hydrophobic elbow and presumably they alter the g120−gp41 interaction to favor receptor binding and/or fusion. In summary, the extreme sensitivity of the gp120-C5 hydrophobic elbow to alanine substitutions suggests that this region is an attractive and novel target for future drug discovery efforts. For example, compounds that bind to gp120-C5 may be expected to disrupt gp120 function and hence HIV entry, either by disrupting gp160 processing or gp120-mediated receptor binding and/or membrane fusion.

ACKNOWLEDGMENT

Reagents pNL4-3.Luc.R-E-, pHXB2-env, U87.CD4.CXCR4, and HIV-1 gp41 hybridoma (Chessie 8) were obtained through the NIH AIDS Research and Reference Program.

REFERENCES

1. Gallo, S., Finnegan, C., Viard, M., Raviv, Y., Dimitrov, A., Rawat, S., Puri, A., Durrell, S., and Blumenthal, R. (2003) The HIV Env-mediated fusion reaction. *Biochim. Biophys. Acta 1614*, 36–50.
2. Freed, E., and Martin, M. (1995) The role of human immunodeficiency virus type 1 envelope glycoproteins in virus infection. *J. Biol. Chem. 270*, 23833–23836.
3. Bazan, H., Alkhatib, G., Broder, C., and Berger, E. (1998) Patterns of CCR5, CXCR4, and CCR3 usage by envelope glycoproteins from human immunodeficiency virus type-1 primary isolates. *J. Virol. 72*, 4485–4491.
4. Björndal, A., Deng, H., Jansson, M., Fiore, J. R., Colognesi, C., Karlsson, A., Albert, J., Scarlatti, G., Littman, D. R., and Fenyo, E. M. (1997) Coreceptor usage of primary human immunodeficiency virus type 1 isolates varies according to biological phenotype. *J. Virol. 71*, 7478–7487.
5. Chan, D., Fass, D., Berger, J., and Kim, P. (1997) Core structure of gp41 from the HIV envelope glycoprotein. *Cell 89*, 263–273.
6. Weissenhorn, W., Dessen, A., Harrison, S., Skehel, J., and Wiley, D. (1997) Atomic structure of the ectodomain from HIV-1 gp41. *Nature 387*, 426–430.
7. Tan, K., Liu, J.-H., Wang, J.-H., Shen, S., and Lu, M. (1997) Atomic structure of a thermostable subdomain of HIV-1 gp41. *Proc. Natl. Acad. Sci. U.S.A. 94*, 12203–12308.
8. Caffrey, M., Cai, M., Kaufman, J., Stahl, S., Wingfield, P., Gronenborn, A., and Clore, G. (1997) Determination of the secondary structure and global topology of the 44 kDa ectodomain of gp41 of the simian immunodeficiency virus by multidimensional nuclear magnetic resonance spectroscopy. *J. Mol. Biol. 271*, 819–826.
9. Caffrey, M., Cai, M., Kaufman, J., Stahl, S., Wingfield, P., Covell, D., Gronenborn, A., and Clore, G. (1998) Three-dimensional solution structure of the 44 kDa ectodomain of SIV gp41. *EMBO J. 17*, 4572–4584.
10. Malashkevich, V., Chan, D., Chutkowski, C., and Kim, P. (1998) Crystal structure of the simian immunodeficiency virus (SIV) gp41 core: conserved helical interactions underlie the broad inhibitory activity of gp41 peptides. *Proc. Natl. Acad. Sci. U.S.A. 95*, 9134–9139.
11. Yang, Z., Mueser, T., Kaufman, J., Stahl, S., Wingfield, P., and Hyde, C. (1999) The crystal structure of the SIV gp41 ectodomain at 1.47 Å resolution. *Struct. Biol. 126*, 131–144.
12. Caffrey, M. (2001) Model for the structure of the HIV gp41 ectodomain: insight into the intermolecular interactions of the gp41 loop. *Biochim. Biophys. Acta 1536*, 116–122.
13. Kwong, P., Wyatt, R., Robinson, T., Sweet, R., Sodroski, J., and Hendrickson, W. (1998) Structure of an HIV gp120 envelope glycoprotein in complex with the CD4 receptor and a neutralizing human antibody. *Nature 393*, 648–659.
14. Huang, C., Tang, M., Zhang, M., Majeed, S., Montabana, E., Stanfield, R., Dimitrov, D., Korber, B., Sodroski, J., and Wilson, I. (2005) Structure of a V3-containing HIV-1 gp120 core. *Science 310*, 1025–1028.
15. Chen, B., Vogan, E., Gong, H., Skehel, J., Wiley, D., and Harrison, S. (2005) Structure of an unliganded simian immunodeficiency virus gp120 core. *Nature 433*, 834–841.
16. Ivey-Hoyle, M., Clark, R., and Rosenberg, M. (1991) The NH_2-terminal 31 amino acids of human immunodeficiency virus type-1

envelope protein gp120 contain a potential gp41 contact site. *J. Virol. 65*, 2682–2685.
17. Helseth, E., Olshevsky, U., Furman, C., and Sodroski, J. (1991) Human immunodeficiency virus type 1 gp120 envelope glycoprotein regions important for association with the gp4 L transmembrane glycoprotein. *J. Virol. 65*, 2119–2123.
18. Binley, J., Sanders, R., Clas, B., Schuelke, N., Master, A., Guo, Y., Kajumo, F., Anselma, J., Maddon, P., Olson, W., and Moore, J. (2000) A recombinant human immunodeficiency virus type 1 envelope glycoprotein complex stabilized by an intermolecular disulfide bond between the gp120 and gp41 subunits is an antigenic mimic of the trimeric virion-associated structure. *J. Virol. 74*, 627–643.
19. Guilhaudis, L., Jacobs, A., and Caffrey, M. (2002) Solution structure of the HIV gp120 C5 domain. *Eur. J. Biochem. 269*, 4860–4867.
20. Page, K., Landau, N., and Littman, D. (1990) Construction and use of a human immunodeficiency virus vector for analysis of virus infectivity. *J. Virol. 64*, 5270–5276.
21. Connor, R., Chen, B., Choe, S., and Landau, N. (1995) Vpr is required for efficient replication of human immunodeficiency virus type-1 in mononuclear phagocytes. *Virology 206*, 935–944.
22. Abacioglu, Y. H., Fouts, T. R., Laman, J. D., Claassen, E., Pincus, S. H., Moore, J. P., Roby, C. A., Kamin-Lewis, R., and Lewis, G. K. (1994) Epitope mapping and topology of baculovirus-expressed HIV-1 gp160 determined with a panel of murine monoclonal antibodies. *AIDS Res. Hum. Retroviruses 10*, 371–381.
23. Douglas, N., Munro, G., and Daniels, R. (1997) HIV/SIV glycoproteins: structure-function relationships. *J. Mol. Biol. 273*, 122–149.
24. McCune, J. M., Rabin, L. B., Feinberg, M. B., Lieberman, M., Kosek, J. C., Reyes, G. R., and Weissman, I. L. (1988) Endoproteolytic cleavage of gp160 is required for the activation of human immunodeficiency virus. *Cell 53*, 55–67.
25. Freed, E. O., Myers, D. J., and Risser, R. (1989) Mutational analysis of the cleavage sequence of the human immunodeficiency virus type 1 envelope glycoprotein precursor gp160. *J. Virol. 63*, 4670–4675.
26. Bosch, V., and Pawlita, M. (1990) Mutational analysis of the human immunodeficiency virus type 1 env gene product proteolytic cleavage site. *J. Virol. 64*, 2337–2344.
27. Jacobs, A., Sen, J., Rong, L., and Caffrey, M. (2005) Alanine scanning mutagenesis of the HIV gp41 loop. *J. Biol. Chem. 280*, 27284–27288.
28. Sen, J., Jacobs, A., Jiang, H., Rong, L., and Caffrey, M. (2007) The disulfide bond is critical to the furin recognition site of HIV gp160. *Protein Sci. 16*, 1236–1241.
29. Schenten, D., Marcon, L., Karlsson, G., Parolin, C., Kodama, T., Gerard, N., and Sodroski, J. (1999) Effects of soluble CD4 on simian immunodeficiency virus infection of CD4-positive and CD4-negative cells. *J. Virol. 73*, 5373–5380.
30. Abrahamyan, L., Markosyan, R., Moore, J., Cohen, F., and Melikyan, G. (2003) Human immunodeficiency virus type 1 Env with an intersubunit disulfide bond engages coreceptors but requires bond reduction after engagement to induce fusion. *J. Virol. 77*, 5829–5836.
31. Binley, J., Cayanan, C., Wiley, C., Schulke, N., Olson, W., and Burton, D. (2003) Redox-triggered infection by disulfide-shackled human immunodeficiency virus type 1 pseudovirions. *J. Virol. 77*, 5678–5684.

BI800227Z